Electronic Supplementary Material (ESI) for Journal of Materials Chemistry A.

Supporting Information

High-Performance Anthraquinone with Potentially Low Cost for Aqueous Redox Flow Batteries

Min Wu, Meisam Bahari, Eric M. Fell, Roy G. Gordon, * *Michael J. Aziz**

Table of Contents

Experimental materials:

1,8-dihydroxyanthraquinone (96%), 1,4-dihydroxyanthraquinone (98%) were purchased from Sigma Aldrich. 50 wt. % glyoxylic acid solution was purchased from Acros Organics. All chemicals were used as received.

1,8-dihydroxy-2,7-dicarboxymethyl-9,10-anthraquinone (DCDHAQ):

3 g of 1,8-dihydroxyanthraquinone (12.49 mmol) was added to 100 mL 1 M NaOH solution. The mixture was stirred at room temperature for 0.5 h under nitrogen. A portion of $Na_2S_2O_4$ (2.39 g, 13.74 mmol) was added to the mixture to give an orange-red solution. Then an aqueous solution of glyoxylic acid (50%, 3 eq.) was added to the above mixture. The solution was stirred at room temperature for 1 hour. Afterward, another portion of $Na_2S_2O_4$ (2.28 g, 13.1) mmol was added to the solution. The temperature was increased to 80 °C, held for 0.5 h, cooled to room temperature and exposed to air. The solution was subsequently acidified with 2 M HCl to collect the crude solid. The crude compound was washed with DMSO to give an orange solid. Yield: 3.1 g (70%). The ^{1}H NMR spectrum of DCDHAQ is shown in Figure S1.

1,4-dihydroxy-2-carboxymethyl-9,10-anthraquinone (1,4-CDHAQ):

3 g of 1,4-dihydroxyanthraquinone (12.49 mmol) was added to 100 mL 1 M NaOH solution. The mixture was stirred at room temperature for 0.5 h under nitrogen. A portion of $Na_2S_2O_4$ (2.39 g, 13.74 mmol) was added to the mixture to give an orange-red solution. Then an aqueous solution of glyoxylic acid (50%, 1.2 eq.) was added to

the above mixture. The temperature was increased to 80 °C, for 1 h, cooled to room temperature and exposed to air. The solution was subsequently acidified with 2 M HCl to collect the crude solid. The crude compound was washed with DMSO to give a red solid. Yield: 3 g (81%).

The ^{1}H NMR spectrum of 1,4-CDHAQ are shown in Figure S2.

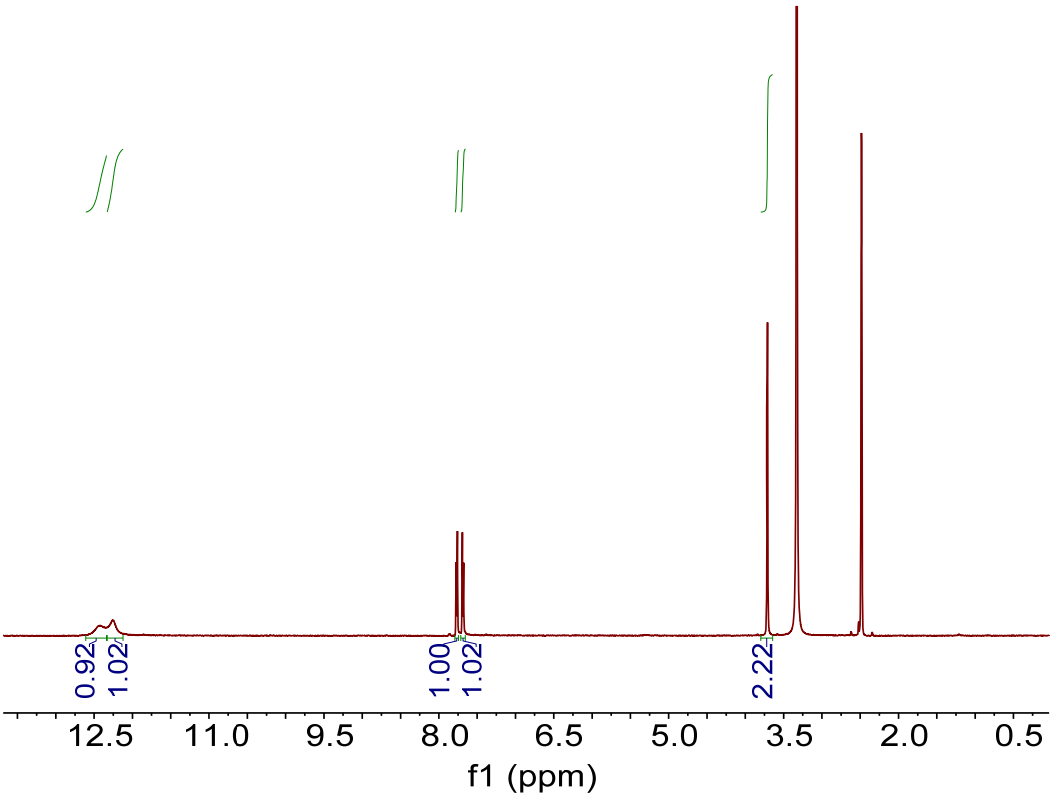

Figure S1. ^{1}H NMR spectrum of DCDHAQ in DMSO-d6. Solvent peaks are those that are not integrated. ^{1}H NMR (500 MHz, DMSO-d_6) δ 12.43 (s, 2H), 12.24. (s, 2H), 7.76 (dd, J=7.5 Hz, 2H), 7.68 (dd, J=7.5 Hz, 2H), 3.71 (s, 4H).

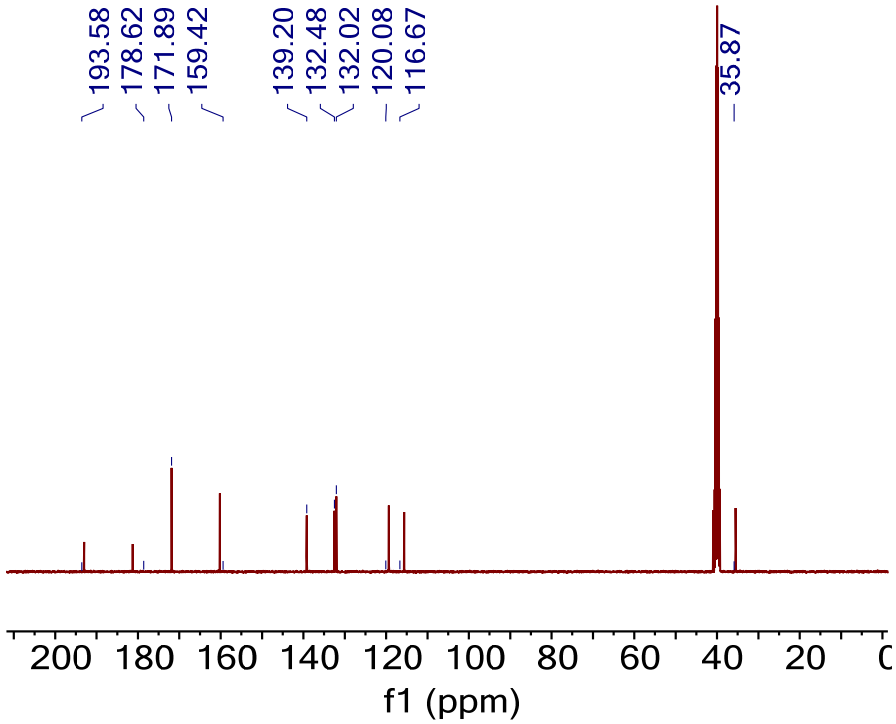

Figure S2. ^{13}C NMR spectrum of DCDHAQ in DMSO-d6. Peaks at 193.58 and 178.62 belongs to the carbons of ketone in anthraquinone core structures, peak at 171.89 is the carboxylic carbon, peak at 35.87 is the methyl carbon of functional chain, other aromatic carbons are similar to the ^{13}C NMR of PEG-AQ reported in *ACS Energy Lett.* 2019, 4, 6, 1342–1348. Note ^{13}C NMR is typically not integrated for quantitative analysis due to the nuclear Overhauser effect.

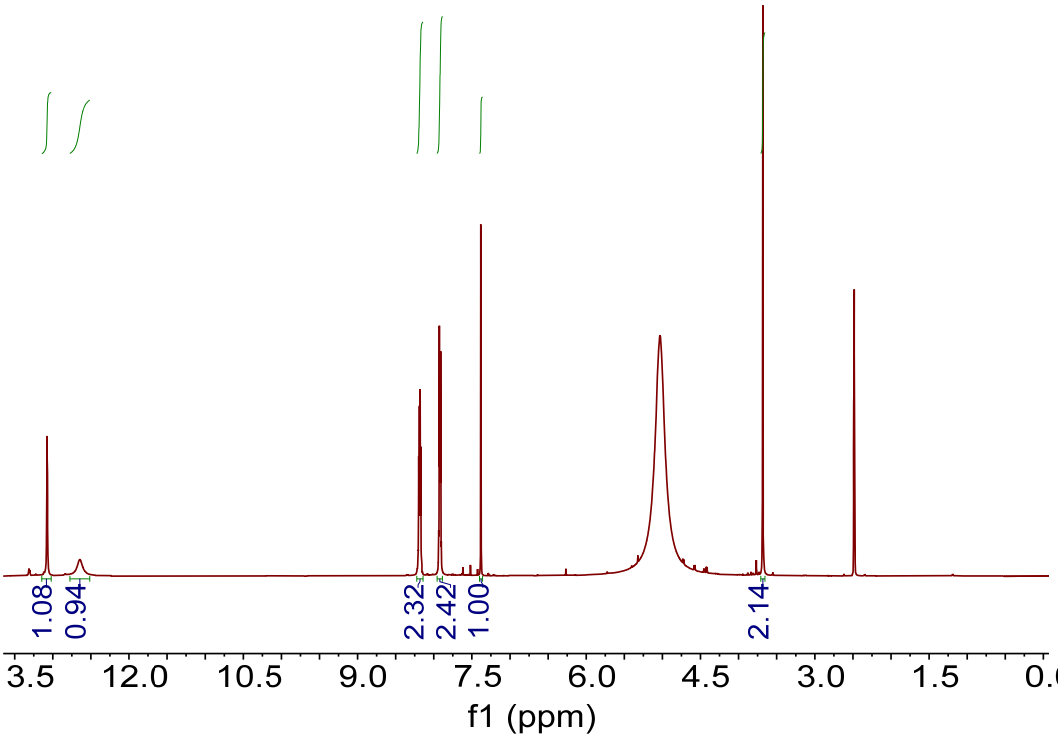

Figure S3. ^{1}H NMR spectrum of 1,4-CDHAQ in DMSO-d6. Solvent peaks are those that are not integrated. ^{1}H NMR (500 MHz, DMSO-d_6) δ 13.10 (s, 1H), 12.66 (s, 1H), 8.22. (m, 2H), 7.95 (m, 2H), 7.42 (s, 1H), 3.70 (s, 2H), peak at 5.02 is the water peak.

Full cell measurements

Flow battery experiments were conducted with cell and hardware from Fuel Cell Tech. (Albuquerque, NM), assembled into a zero-gap flow cell configuration. Pyrosealed POCO graphite flow plates with serpentine flow patterns were used for both electrodes. Each electrode comprised a 5 cm^2 geometric surface area covered by one sheet of AvCarb carbon cloth electrode. For DCDHAQ/ferrocyanide full cell tests, a Nafion^{TM} 212 membrane was used to serve as the ion-selective membrane between the AvCarb electrodes. The Nafion membrane was soaked in 1M KOH for 24 hours before use. The

outer portion of the space between the electrodes was gasketed by Viton sheets with the area over the electrodes cut out. Torque applied during cell assembly was 60 lb-in (6.78 Nm) on each of eight 1/4-28 bolts. The electrolytes were fed into the cell through fluorinated ethylene propylene (FEP) tubing at a rate of 60 mL/min, controlled by Cole-Parmer 6 Masterflex L/S peristaltic pumps. The 0.2 M DCDHAQ/ferrocyanide cell was run inside a nitrogen-filled glove bag and the 0.75 M DCDHAQ/ferrocyanide cell was run inside a glove box (1 ppm O_2). Cell polarization measurements and charge-discharge cycling were performed using a Biologic BCS-815 battery cycler. Long-term cycling of the 0.2 M DCDHAQ/ferrocyanide cell was performed at ±50 mA cm^{-2} with potential holds at 1.4 V for charging and 0.8 V for discharging until the current density dropped to 2 mA cm^{-2}. For the limited SOC cycling, the cell was charged to a fixed state of charge (e.g., 80% SOC or 90% SOC) and then fully discharged to 0.8 V with the potential held until the current dropped to 2 mA cm^{-2}. For the 0.75 M DCDHAQ/ferrocyanide cell, the cut-off voltage was 1.4 V for charging and 0.6 V for discharging. The polarization curves were obtained by charging to the desired state of charge first and then polarizing via linear sweep voltammetry at a rate of 100 mV s^{-1}. This method yielded polarization curves very close to those obtained by point-by-point galvanostatic holds and imposes minimal perturbation to the SOC of the small-electrolyte-volume cell.

A glassy carbon (BASi, 3 mm diameter) working electrode, an Ag/AgCl reference electrode (BASi, pre-soaked in a 3 M NaCl solution), and a graphite counter electrode were used in the three-electrode system for all CV tests.

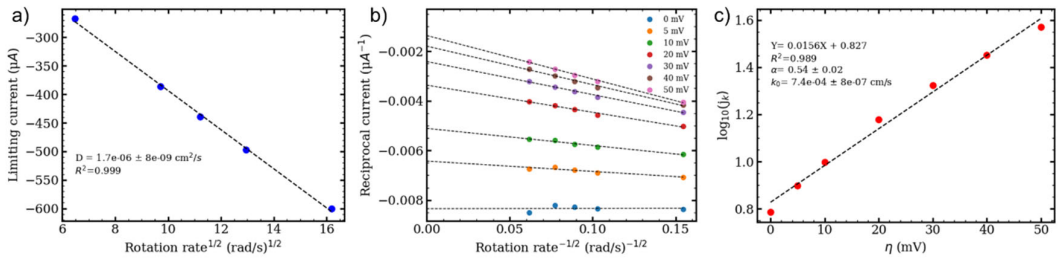

Figure S4. Electrochemical kinetics of DCDHAQ at pH 14. a) Levich plot (limiting current versus square root of rotation rate) of 5 mM DCDHAQ in 1 M KOH. Limiting current is taken as the current at -0.8 V vs SHE in Figure 1d. The slope yields a diffusion coefficient for the oxidized form of DCDHAQ of 1.7×10^{-6} cm^2/s. b) Koutecký-Levich plot (reciprocal current versus inverse square root of rotation rate) of 5 mM DCDHAQ in 1 M KOH. c) Fitted Tafel plot of 5 mM DCDHAQ in 1 M KOH. The charge transfer coefficient is calculated to be 0.54, and the rate constant is calculated to be 7.4×10^{-4} cm/s.

Table S1. Properties and cycling parameters of aqueous RFBs utilizing potentially low-cost redox-active organics, i.e. organic or metalorganic molecules that do not require multiple synthetic steps or expensive precursors.

Negolyte	Posolyte	Electron Concentration (M) Nego-/Posolyte	$E_{cell} - E^{0'}_{cell}$ (V)	Cut-off current density (mA/cm^2)	Cell voltage (V)	Capacity fade rate (%/day)	Ref.
Methyl viologen	4-OH-TEMPO	0.5/0.5	0.45	60	1.25	3.5	1
Methyl viologen	FcNCl	0.7/0.7	0.45	60	1.06	1.3	2
Alloxazine ACA	Ferrocyanide	2/0.4	0.6	100	1.13	1.8	3
DHPS	Ferrocyanide	2.8/0.31	0.3	100	1.4	0.68	4
Phenazine BHPC	Ferrocyanide	1/0.4	0.4	100	1.3	0.08	5
2,6-DHAQ	Ferrocyanide	1/0.4	0.5	100	1.2	5	6
1,8-DHAQ	Ferrocyanide	0.2/0.2	0.45	80	1.1	13	7
PEGAQ	Ferrocyanide	3/0.31 0.2/0.1	0.25	16	1.05	0.5 1.1	8
$(SPr)_2V$	Ferrocyanide	0.5/0.5 0.9/0.9	0.38	80	0.82	<7.1 <2.7[a]	9
DCDH-AQ	Ferrocyanide	1.5/0.3 0.4/0.2	0.35	2	1.1	0.03 0.1	**This work**

[a]A capacity fade rate of 0 is claimed. However, both species comprise both sides of a symmetric cell, cycling is purely galvanostatic, extensive crossover is reported and, for the high concentration case, only 77.5% of theoretical capacity of one side is accessed. The possibility that additional capacity is recruited by crossover from the side on which it is inactive to make up for species loss on the side on which it is active is not excluded. Apparent capacity remains stable at ~77.5% of theoretical for ~1100 hr; thus, true capacity fade rate < (200%-77.5%)/1100 hr = 2.7%/day. Likewise, the low concentration case accessed 82% of theoretical capacity for 400 hr, leading to an upper limit of 7.1%/day.

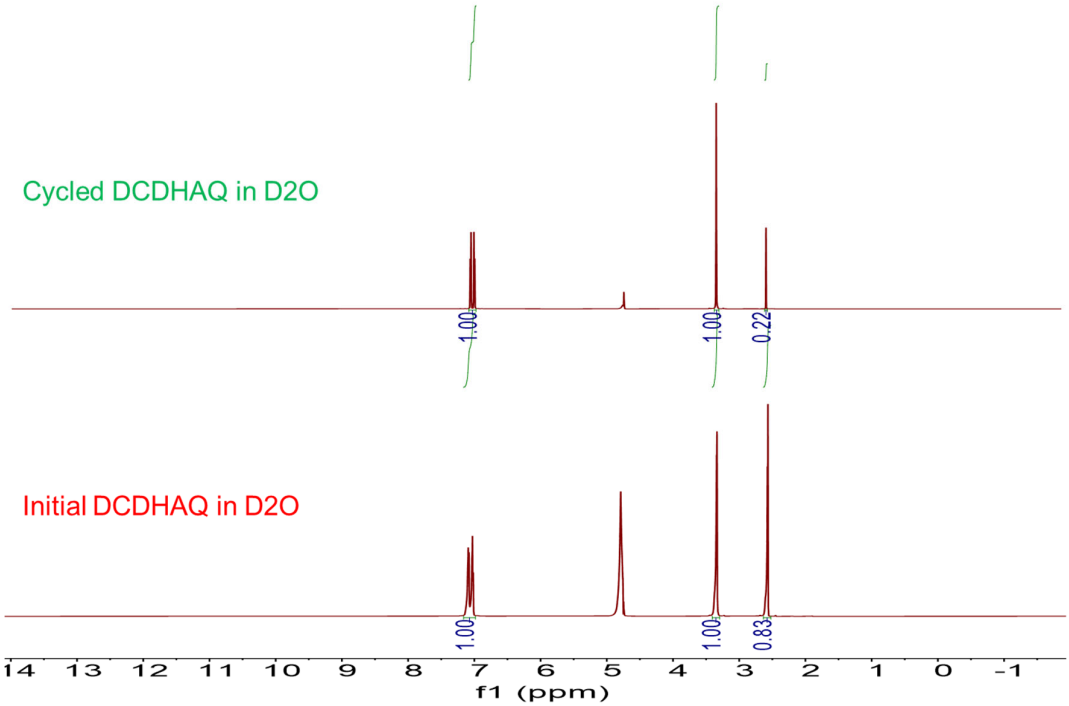

Figure S5. ^{1}H NMR of initial DCDHAQ and cycled DCDHAQ in D_2O solvent. The cycled 0.75 M DCDHAQ from the long cell cycling test was diluted with D_2O solvent with a volume ratio of 1:5. Suppression of the peak from water at 4.7 ppm was performed to increase other signals. No new decomposition peaks were observed. Peaks at 7.06 and 3.35 belong to DCDHAQ; peak at 2.57 belongs to DMSO, which does not shows up in DMSO-d6 solvent. The DMSO peak decreased because of the crossover of DMSO to the posolyte.

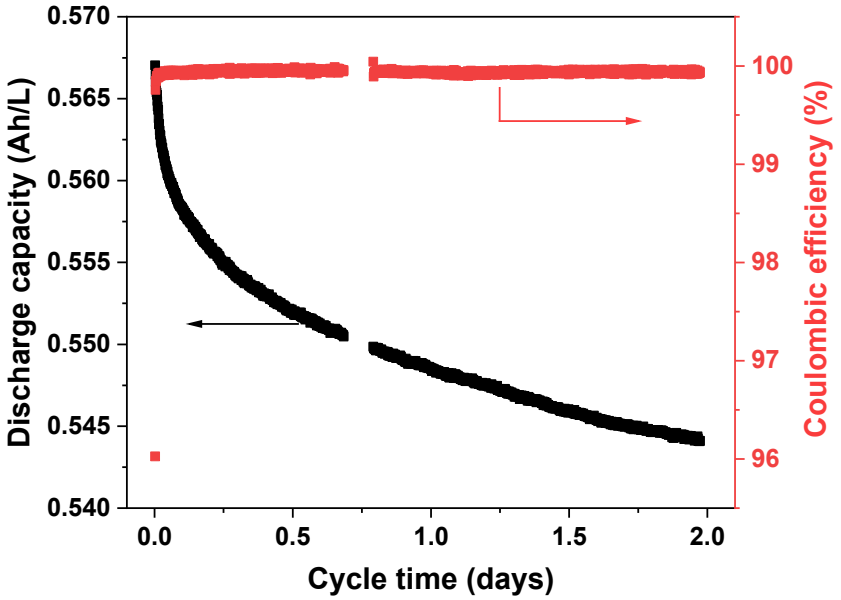

Figure S6. Cell cycling of 6 mL saturated 1,8-DHAQ at pH 14 and 30 mL 0.1 M ferrocyanide + 0.02 M ferricyanide at pH 14. The cell was cycled between 0.8-1.4 V with a potential hold till current dropped to 2 mA/cm2. Nafion 212 was used as the membrane and untreated AvCarb carbon electrode was used as the electrode.

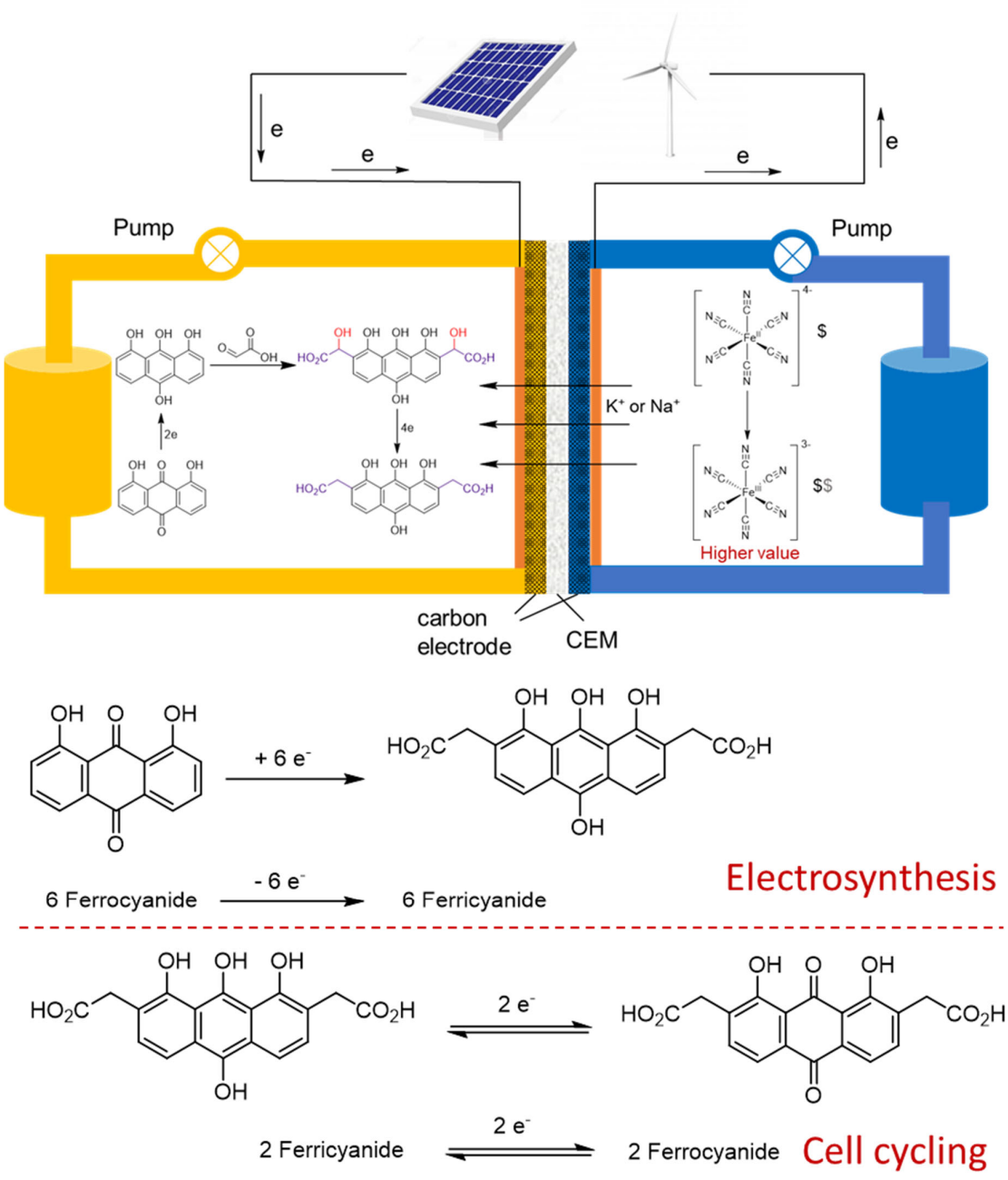

Figure S7. Proposed electrochemical synthesis method for DCDHAQ.

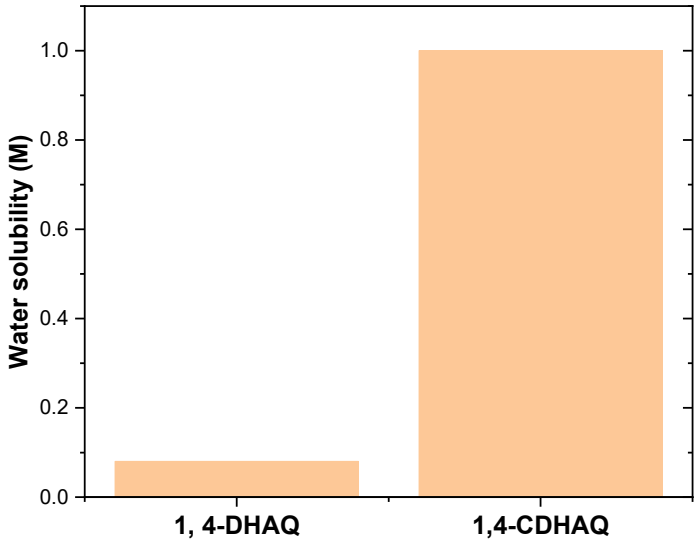

Figure S8. Water solubility comparison for 1,4-DHAQ and 1,4-CDHAQ in 1 M KOH (aq).

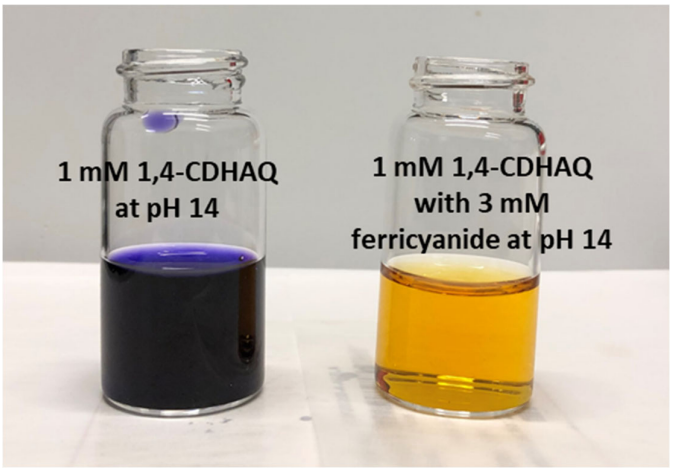

Figure S9. Photo of 1 mM 1,4-CDHAQ (purple color) at pH 14 and 1 mM 1,4-CDHAQ with 3 mM potassium ferricyanide at pH 14 (yellow color).

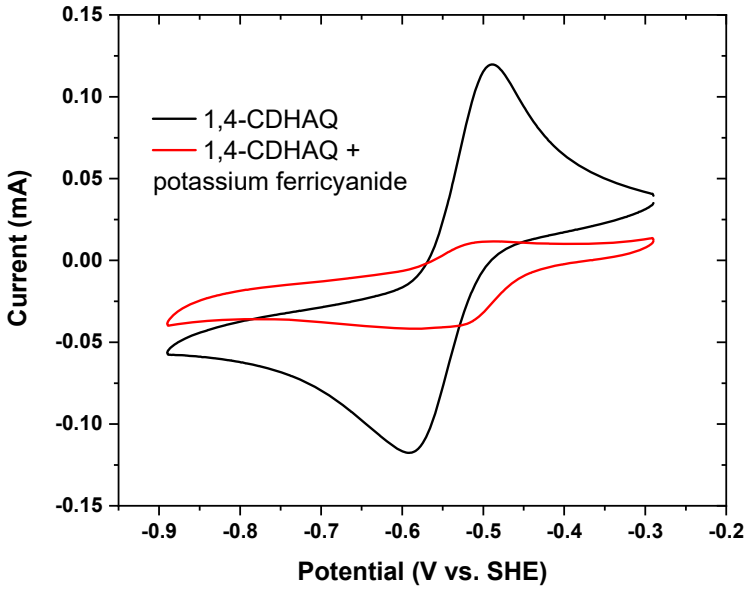

Figure S10. Cyclic voltammograms of 5 mM 1,4-CDHAQ at pH 14 and a solution of 5 mM 1,4-CDHAQ with 12 mM potassium ferrocyanide at pH 14 with a scan rate of 100 mV/s.

Table S2. Electrochemical, physical properties, and estimated cost comparison between 1,8-DHAQ, 2,6-DHAQ, 2,6-DBEAQ, DPivOHAQ, DCDHAQ, 1,4-DHAQ. The lab-scale cost of 1,8-DHAQ, 2,6-DHAQ and 1,4-DHAQ are from Sigma-Aldrich in December 2020. The estimated mass-production costs are from refs. [10] and [11]. DCDHAQ combines the high stability and potential low cost traits.

Compounds	Solubility (Mol L^{-1}) pH = 14	$E_{1/2}$ (V vs. SHE) at pH 14	Capacity Fade Rate (%/Day)	Lab-Scale Cost ($/$Mol_{e^-}$)	Estimated Mass-Production Cost ($/kAh)
1,8-DHAQ	0.01	-0.58	0.85-4	34	N/A
2,6-DHAQ	0.6	-0.67	5	3240	26 [ref.10]
2,6-DBEAQ	1.1	-0.52	0.04[a]	N/A	81-111 [ref.10]
DPivOHAQ	1	-0.48	0.014[a]	N/A	147 [ref.10]
DCDHAQ	1.3	-0.56	0.03-0.1	82	41-53 [ref.11]
1,4-DHAQ	0.08	-0.56	N/A	23	20 [ref.11]

[a] Note: capacity fade rate comes from cycling at pH 12. For those unspecified cases, the capacity fade rate comes from cycling at pH 14.

Estimation of cost of electrolytes

The cost of 1 kg of 50 wt. % glyoxylic acid solution at Sigma-Aldrich is $104, corresponding to $15.4/mol. Therefore, the lab-scale cost of DCDHAQ is estimated to be (34*2+3*15.4)/2/70% = $82/mol electrons without considering the cost of KOH and sodium dithionite as they are quite inexpensive and also could be potentially eliminated by the electrochemical synthesis proposed in the main text. In the arithmetic, 2 means two electrons per anthraquinone molecule, 3 means three equivalent of side chain

precursor used for synthesis, and 70% is the synthetic yield. The estimated lab-scale cost of DCDHAQ is slightly higher than that of 1,8-DHAQ but significantly lower than that of 2,6-DHAQ.

The mass-production cost of 2,6-DHAQ was estimated to be \$5.8/kg.[11] Thus, we suppose the scalable cost of DCDHAQ could be significantly below \$10/kg, resulting in a capacity cost of <\$66/kAh for the 2-electron DCDHAQ in the negolyte. Indeed, a recent cost-of-manufacture estimate from Borealis Technology Solutions, LLC, using a similar approach to that in Ref. 11 and starting with a price quote for 1,4-DHAQ, yielded a cost of \$7.8/kg (\$52/kAh) at a scale of 100,000 metric tonnes per year via the chemical synthesis route and \$6.2/kg (\$41/kAh) at a scale of 100,000 metric tonnes per year via the electrosynthesis route[11]. Similarly, if we start with the cost for 2,6-DHAQ, then the cost for DCDHAQ is around \$8/kg (\$53/kAh) via the electrosynthesis route. Because the lab-scale cost for 1,8-DHAQ is between those of 2,6-DHAQ and 1,4-DHAQ, it is reasonable to suppose the production cost could be in the range of \$41-53/kAh.

Discussion of the relationship between state of charge, applied cell voltage and cell current

Electrochemical reactions that occur in a flow battery and the relevant equilibrium potentials can be expressed as

$$\text{Posolyte: A - ne}^- \rightleftharpoons \text{A}^{n+}, E^{eq}_{posolyte} = E^{0'}_{posolyte} - \frac{RT}{nF} ln \frac{C^*_A}{C^*_{A^{n+}}}; \quad \text{(S1)}$$

Negolyte: $B + me^- \rightleftharpoons B^{m-}$, $E^{eq}_{negolyte} = E^{0'}_{negolyte} - \frac{RT}{mF} ln \frac{C^*_{B^{m-}}}{C^*_B}$. (S2)

with the assumption that the activity coefficients are concentration-independent. C represents the concentration of the electroactive species A or B either in its reduced or oxidized form. E^{eq} and $E^{0\prime}$ are equilibrium and formal potentials of desired electrolytes as denoted by the relevant subscripts. And *n* and *m* are the number of electrons transferred during the electrochemical reaction of A and B, respectively. The cell potential becomes

$$E_{cell} = E^{eq}_{posolyte} - E^{eq}_{negolyte} + ir(i) = E^{0'}_{cell} - \frac{RT}{nF} ln \frac{C^*_A}{C^*_{A^{n+}}} + \frac{RT}{mF} ln \frac{C^*_{B^{m-}}}{C^*_B} + ir(i), \quad \text{(S3)}$$

where E_{cell} is the cell potential, $E^{0'}_{cell}$ is the formal potential difference for the posolyte and negolyte when each are 50% at the reduced state, *ir(i)* is the total cell overpotential, reckoned as positive during the charging step. For an anthraquinone (AQ)/ferrocyanide full cell, *m*=2 and *n*=1 as anthraquinone and ferrocyanide undergo two-electron and one-electron redox processes, respectively. Under a negolyte capacity-limited condition with the assumption that no complexes form in the electrolytes, we have

$$\frac{C^*_{B^{m-}}}{C^*_B} = \frac{SOC}{1 - SOC}$$

(S4)

$$E_{cell} = E^{0'}_{cell} - \frac{RT}{F} ln \frac{C^*_{Ferro}}{C^*_{Ferri}} + \frac{RT}{2F} ln \frac{SOC}{1 - SOC} + ir(i). \quad \text{(S5)}$$

In a general case of AQ as the capacity limiting side,

$$\frac{C^*_{Ferro}}{C^*_{Ferri}} = \frac{n^0_{Ferro} - 2n_{rAQ}}{n^0_{Ferri} + 2n_{rAQ}} = \frac{n^0_{Ferro} / 2n^0_{AQ} - 2n_{rAQ} / 2n^0_{AQ}}{n^0_{Ferri} / 2n^0_{AQ} + 2n_{rAQ} / 2n^0_{AQ}} = \frac{p - SOC}{q + SOC}, \quad \text{(S6)}$$

where $n^0_{Ferro}, n^0_{Ferri}, n^0_{AQ}$ are the initial molarities of ferrocyanide, ferricyanide, and total molarities of AQ (reduced + oxidized); and n_{rAQ} is the molarity of reduced AQ. p and q represent the initial capacity ratios of ferrocyanide to AQ and ferricyanide to AQ, respectively, and are defined as:

$$p = n^0_{Ferro} / 2n^0_{AQ}; \tag{S7}$$

$$q = n^0_{Ferri} / 2n^0_{AQ}. \tag{S8}$$

Therefore, the cell potential, E_{cell}, of an AQ capacity-limited flow battery may be expressed as:

$$E_{cell} = E^{0'}_{cell} + \frac{RT}{2F} ln\left(\frac{SOC}{1-SOC} \times \left(\frac{q+SOC}{p-SOC} \right)^2 \right) + ir(i). \tag{S9}$$

For a capacity-balanced full cell for which the capacity of posolyte and negolyte are equal, p=1 and q=0. We plot effective Nernstian voltage $E_{cell} - E^{0'}_{cell} - ir(i)$ as a function of SOC at different electrolyte compositions to obtain **Figure 2**.

Supplemental References

[1] T. B. Liu, X. L. Wei, Z. M. Nie, V. Sprenkle, W. Wang, *Adv. Energy Mater.* **2015**, *6*, 1501449.

[2] B. Hu, C. DeBruler, Z. Rhodes, T. L. Liu, *J. Am. Chem. Soc.* **2017**, *139*, 1207.

[3] K. Lin, R. Gomez-Bombarelli, E. S. Beh, L. Tong, Q. Chen, A. Valle, A. Aspuru-Guzik, M. J. Aziz, R. G. Gordon, *Nat. Energy* **2016**, *1*, 16102.

[4] A. Hollas, X. L. Wei, V. Murugesan, Z. M. Nie, B. Li, D. Reed, J. Liu, V. Sprenkle, W. Wang, *Nat. Energy* **2018**, *3*, 508.

[5] C. Wang, X. Li, B. Yu, Y. Wang, Z. Yang, H. Wang, H. Lin, J. Ma, G. Li, Z. Jin, *ACS Energy Lett.* **2020**, *5*, 411.

[6] K. Lin, Q. Chen, M. R. Gerhardt, L. Tong, S. B. Kim, L. Eisenach, A. W. Valle, D. Hardee, R. G. Gordon, M. J. Aziz, M. P. Marshak, *Science* **2015**, *349*, 1529.

[7] J. Y. Cao, M. Tao, H. P. Chen, J. Xu, Z. D. Chen, *J. Power Sources* **2018**, *386*, 40.

[8] S. Jin, Y. Jing, D. G. Kwabi, Y. Ji, L. Tong, D. De Porcellinis, M. A. Goulet, D. A. Pollack, R. G. Gordon, M. J. Aziz, *ACS Energy Lett.* **2019**, *4*, 1342.

[9] J. Luo, B. Hu, C. Debruler, Y. Bi, Y. Zhao, B. Yuan, M. Hu, W. Wu, T. L. Liu, *Joule*, 2019, *3*(1), 149-163.

[10] T. D. Gregory, M. L. Perry, P. Albertus, *J. Power Sources*, **2021**, *499*, 229965.

[11] T.D. Gregory (private communication).